Adsorption geometry of Cu(111)-Cs studied by scanning tunneling microscopy

Th. von Hofe, J. Kröger,* and R. Berndt
Institut für Experimentelle und Angewandte Physik,
Christian-Albrechts-Universität zu Kiel, D-24098 Kiel, Germany

Using scanning tunneling microscopy at low temperatures we investigated cesium adsorbed on Cu(111). At low coverages we observe a hexagonally ordered Cs adsorption layer with a mutual adsorbate distance of 1.1 nm. This distance is discussed in terms of a commensurate adsorption superstructure which is stabilized by long-range adsorbate interactions mediated by Cu(111) surface state electrons. Intermediate coverages are characterized by incommensurate superstructures which are rotated with respect to the substrate lattice. The rotation angle varies with coverage and follows a trend which is consistent with models of epitaxial rotation. With increasing coverage the adsorption layers are found to rotate toward alignment with the substrate.

PACS numbers: 06.30.Bp,68.37.Ef,68.55.Jk

I. INTRODUCTION

A. Alkali metal adsorption on metal surfaces

Investigations of the adsorption of alkali metals on single-crystal metal surfaces has a long tradition in surface science. This is partly due to potential technological applications like the promotion of catalytic reactions, an enhanced oxidation,[1,2,3,4] and an increase in electron emission rates.[5,6] Moreover alkali metal atoms are, due to their simple electronic structure, candidates for model chemisorption studies as reviewed, for instance, in Refs. 7 and 8. Recently published articles[9,10,11,12,13] focus on the investigation of electronic and dynamic properties of Cs layers on Cu(111). Consequently, it is important to study the geometrical structure of this adsorbate system. Before addressing the particular adsorbate system Cu(111)-Cs we give a general overview of alkali metals adsorbed on surfaces. An excellent review on this subject has been given by Diehl and McRath.[14]

Structural characterization of alkali adsorbate systems has been a central issue and resulted in the following general picture of alkali adsorption on metal surfaces. Due to charge transfer from the adsorbed alkali atom to the substrate, the alkali adatoms become partially charged.[15] The induced dipole moment then causes the alkali atoms to mutually repel leading to homogeneous adatom arrangement. As a result, at very low coverages low-energy electron diffraction (LEED) patterns reveal a ring around the (0,0) spot.[16,17,18,19,20] The formation of such structures in LEED patterns indicates a superstructure of randomly distributed adsorbed atoms (adatoms) with a prevailing mutual distance. In contrast, higher coverages lead to sharp diffraction spots indicating a periodic superstructure with long-range order. At room temperature, superstructures were observed only for commensurate phases, *e. g.*, for Co(10$\bar{1}$0)-K,[21] Au(100)-K,[22] and Ni(111)-K.[23] Below room temperature, incommensurate phases were reported, for instance, for Ag(111)-K, -Rb, -Cs,[20] and Ni(100)-K.[24] Rotation of an incommensurate adsorption layer (adlayer) with respect to the substrate, with the rotation angle depending continuously on the coverage, was observed for various systems, namely C(0001)-Cs,[25] Pt(111)-Na,[17] Pt(111)-K,[26] Ru(0001)-Li,[27] Ru(0001)-Na,[28] Ag(111)-K, -Rb, -Cs,[20] Cu(100)-K and Ni(100)-K,[24], and Rh(100)-Cs.[29] Models which describe the rotational behavior are based on domain wall alignment with a symmetry direction of the substrate,[30,31,32] higher-order commensurate phases,[33] or response of an elastic overlayer to a small-amplitude corrugation of the substrate potential.[34,35]

Few alkali-substrate combinations lead to island formation at coverages below saturation, like Al(111)-Na, -K, -Rb,[36,37] Al(100)-Na,[38,39] Cu(111)-Na,[40] Cu(100)-Li,[41] Cu(100)-K,[42], and Ag(100)-K.[43] Within the islands, the alkali atoms form commensurate superstructures. A density functional theory study[44,45] indicates that the adsorbate-substrate interactions exceed the repulsive adsorbate-adsorbate interactions at low coverages for these systems. Additionally, these systems condense in (higher-order) commensurate phases which suggests that the energy gain from forming commensurate phases promotes island formation.[14]

For substrate surfaces with square or rectangular symmetry the alkali atoms occupy adsorption sites which maximize the coordination number to the substrate.[38,46,47,48,49,50,51] The on-top adsorption site is frequently observed for hexagonally close-packed substrate surfaces, for instance, Cu(111)-p(2 × 2)Cs,[52] Al(111)-($\sqrt{3}\times\sqrt{3}$)Rb,[53] and Ni(111)-p(2×2)K[54] to name only a few, and bridge site for Rh(111)-p(2×2)Rb.[55] For the systems with on-top-site adsorption, LEED studies showed that the adatoms push their supporting atom below the surface layer leading to surface rumpling and an increase of the coordination number.[14]

B. Cs on Cu(111)

Two publications report the geometrical structure of Cs adsorbed on Cu(111). Lindgren *et al.* inferred from LEED investigations[52] that room-temperature adsorption of Cs on Cu(111) leads to a saturation coverage.

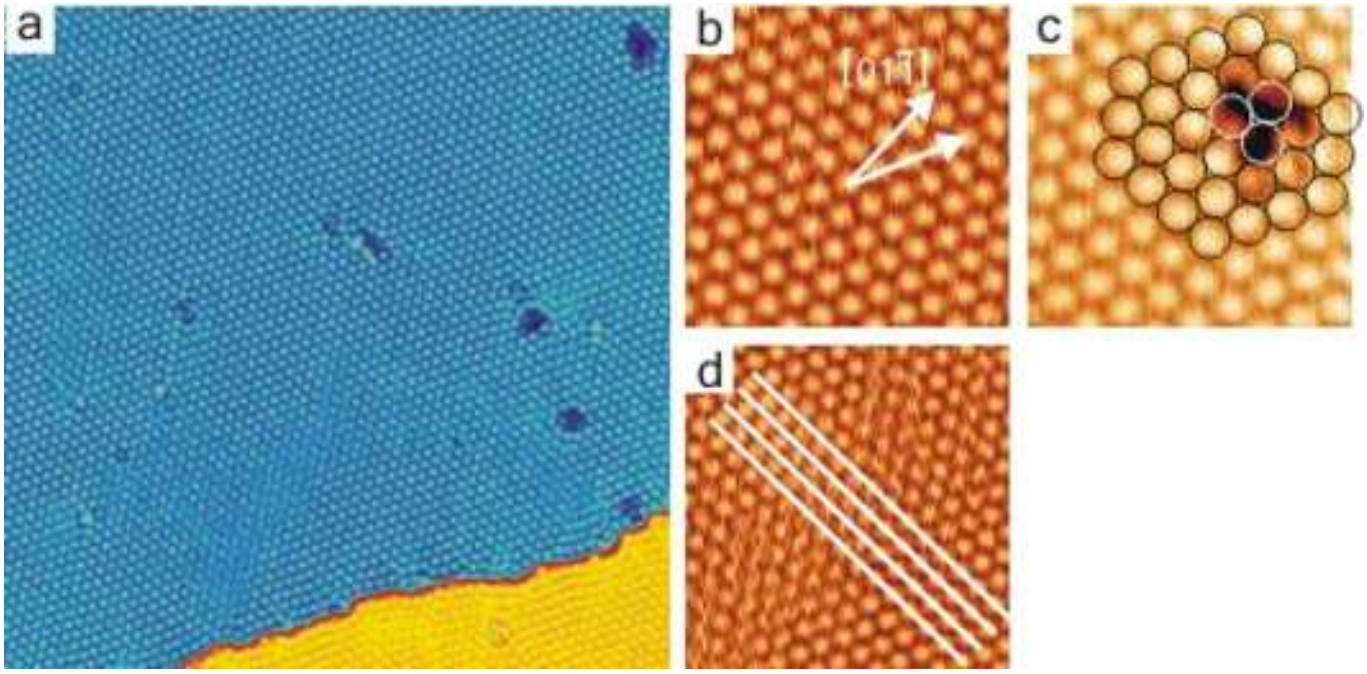

FIG. 1: (Color online) a) Constant-current STM image of the Cu(111)-Cs surface at 0.05 ML. The bright circular protrusions are assigned to single Cs atoms. (58 nm × 58 nm, tunneling parameters: $V = -600$ mV, $I = 0.1$ nA; fast scan direction is from top to bottom.) b) Close-up view of an area of 10 nm × 10 nm. The indicated [01$\bar{1}$] direction corresponds to a close packing direction of the substrate ($V = -600$ mV, $I = 0.1$ nA). c) Close-up view (9 nm × 9 nm) contains a defect in the top right corner of the image. The black circles indicate the position of adjacent Cs atoms, while the white circles continue this hexagonal lattice also inside the defect structure. d) Close-up view (14 nm × 14 nm) indicating that two adjacent Cs domains (upper left and lower right quarter) are mutually shifted by half an adatom row.

After completing the first adsorption layer further exposure to Cs did not increase the coverage. This adsorption layer revealed a p(2 × 2) superstructure, with Cs atoms occupying on-top adsorption sites. For lower coverages the ring formation in LEED patterns as described above was observed. Further studies of Cu(111)-Cs were reported by Fan and coworkers.[56] They examined adsorption structures in the temperature range between 80 K and 500 K. As a result the saturation coverage increases to 0.28 ML at 80 K, where 1 ML is defined as one Cs atom per Cu atom. Fan *et al.* did not report any commensurate phase for temperatures down to 80 K except for the already known p(2 × 2) superstructure. However, they reported orientationally ordered incommensurate phases for coverages $\Theta > 0.12$ ML at 80 K.

The cesium-covered Cu(111) surface has attracted much interest recently. Excited Cs states in the low-coverage regime have been investigated by time-resolved two-photon photoemission experiments to gain insight into the bonding and electronic relaxation of alkali atoms on metal surfaces.[9,10] The dynamics of quantum well states, which are localised in the ultrathin Cs layer on Cu(111), have recently been investigated by a combined theoretical and tunneling spectroscopy study.[13] Surprisingly, in spite of the substantial interest in their dynamic and electronic properties a real-space analysis of the geometric structure of Cs films on Cu(111) at various coverages is still lacking. In this article we present the results of a scanning tunneling microscopy (STM) study of Cu(111)-Cs for different coverages at 9 K. Atomic resolution of the Cs adlayer reveals incommensurate phases, which are rotated with respect to the Cu(111) lattice. The rotation angle decreases with increasing coverage and vanishes at the p(2 × 2) superstructure. At very low coverages a commensurate phase is found, which exhibits mutual Cs distances of 1.1 nm. This distance suggests an electronic stabilization of the adsorbate lattice: Adsorbate-induced Friedel oscillations of the substrate charge density provided by the Cu(111) surface state give rise to an adsorbate-adsorbate distance corresponding to half the Fermi wavelength of surface-state electrons.

II. EXPERIMENT

The experiments were performed in ultrahigh vacuum recipients with a base pressure of 10^{-8} Pa. The homemade scanning tunneling microscope was operated at room temperature and at 9 K. Clean Cu(111) surfaces were obtained after several cycles of argon ion bombardment and annealing. Crystalline order and adsorbate superstructures were monitored with LEED and cleanliness was checked with STM. The clean Cu(111) surface was exposed to Cs at room temperature. Cesium was evapo-

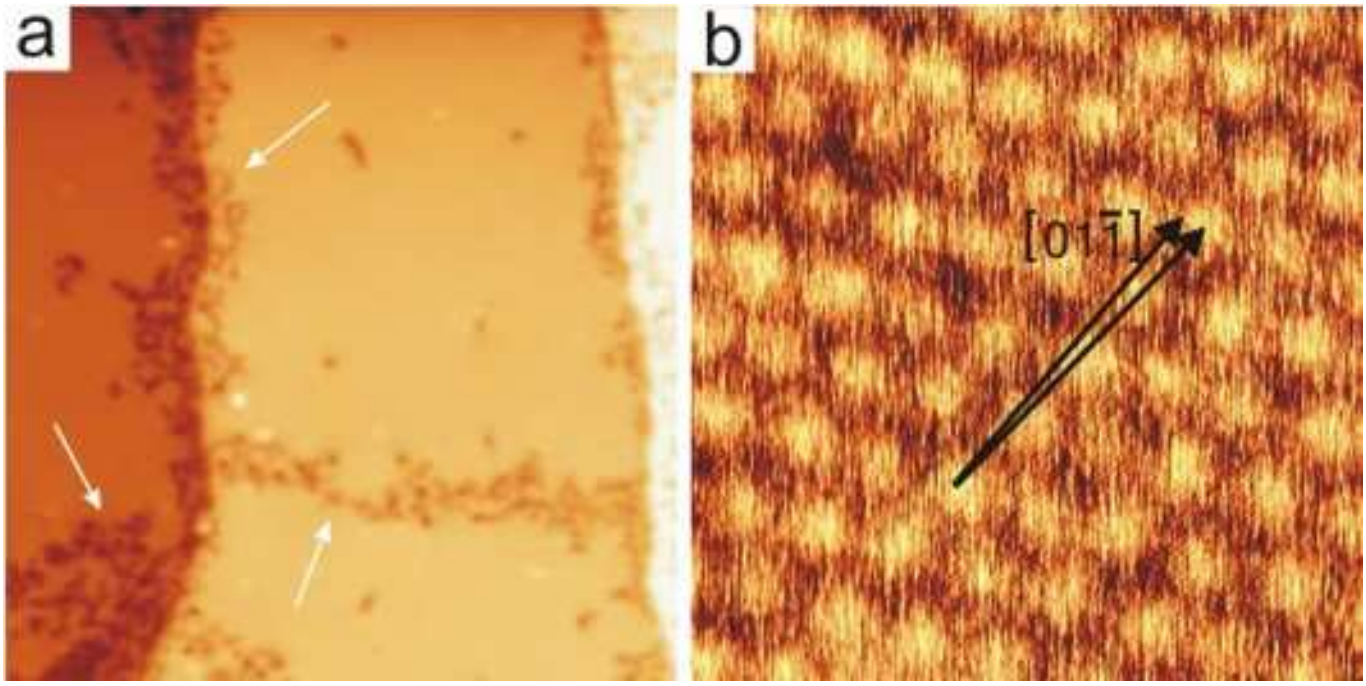

FIG. 2: (Color online) a) Constant-current STM image of Cu(111)-Cs at 0.18 ML. The Cs layer is almost closed, only at step edges and occasionally inside the layer, irregularly formed patterns (marked by arrows) are observed (62 nm × 62 nm, $V = 200$ mV, $I = 0.1$ nA). b) Close-up view of a scan area inside the closed Cs layer displayed in a. The bright circular protrusions are assigned to single Cs atoms. Crystallographic orientation of Cu(111) is indicated (4.5 nm × 4.5 nm, $V = 50$ mV, $I = 0.1$ nA).

rated from a commercial dispenser[57] keeping the pressure below 5×10^{-8} Pa. Using a quartz microbalance the deposition rate was monitored to be ≈ 0.06 ML min^{-1}. We define the coverage as the number of Cs atoms per Cu atom, *i. e.*, one Cs atom per Cu atom corresponds to one monolayer (ML). The saturation coverage of Cs at room temperature corresponds to the p(2 × 2) superstructure with a coverage of 0.25 ML. This definition follows Fan *et al.*[56] and deviates from the one used by Lindgren and coworkers[52] where the saturation coverage is defined as 1 ML. We find that further exposure does not lead to an increase of the surface coverage in agreement with the results of Ref. 52. The directions of close-packed atoms of the Cu(111) surface were obtained by analyzing LEED diffraction patterns with an accuracy of 2°.

We noticed that during extended LEED measurements of Cu(111)-p(2×2)Cs the superstructure diffraction spots became less intense and less sharp when using electron kinetic energies in excess of 100 eV on a timescale of 1 h. The dynamic LEED experiments by Lindgren *et al.*[52] should not be affected by this kind of e-beam damage since the maximum electron energy in their experiments was 150 eV and the measurements were performed within a few minutes.

III. RESULTS

Typical constant-current STM images of Cu(111)-Cs acquired at room temperature (not shown) do not reveal any adsorbate superstructure. We inferred the presence of the adsorbate from a noisy tunneling current, which we do not usually observe on clean metal surfaces. Further, step edges were not imaged as straight lines. Rather, step edges appear frayed in constant-current STM images. We attribute these observations to mobility and to tip-induced movements of the Cs adatoms. Due to the instability of the tunneling junction, tunneling spectroscopy measurements were difficult to perform in a reproducible manner at room temperature. As a consequence we performed our experiments at 9 K. The data to be presented in the following were acquired at low temperature.

A. Low coverage: $\Theta = 0.05$ ML

Figure 1a shows a representative constant-current STM image of Cu(111) covered with 0.05 ML Cs revealing an area of more than 2500 nm^2 with a step crossing in the lower right. Hexagonally ordered bright circular protrusions cover the whole image. We observed this superstructure for many different areas of the sample. The close-up view in Fig. 1b shows the hexagonal Cs super-

lattice in more detail. From this image an interatomic distance of 1.1 nm can be determined. The corrugation of the superlattice is ≈ 0.03 nm. The arrows indicate directions of close packing of the Cu(111) substrate ($[01\overline{1}]$) and of the adlayer. Evidently the Cs layer is rotated by $\approx 23°$ with respect to the Cu(111) surface. On the right side of Fig. 1a defects of the adsorption layer are observed. We attribute these defects to imperfections of the Cs layer, *i. e.*, to missing Cs adatoms. To corroborate this assumption a close-up view of the defect in the upper right corner of Fig. 1a is shown in Fig. 1c. The black circles indicate the positions of Cs atoms in the layer, while the white circles continue the hexagonal lattice inside the defect structure. From this image we infer that the dark area corresponds to missing Cs atoms.

The hexagonal order of the adatoms extends over large areas. In some regions, atomic resolution of the adsorbate layer is lost during scanning. These regions appear as blurred stripes in the fast scanning direction (from top to bottom in Fig. 1d). In $\approx 40\,\%$ of the cases where the blurred stripes appear, adjacent Cs-covered areas are shifted with respect to each other by half a superlattice constant as indicated by white lines in Fig. 1d. We attribute this observation to adjacent Cs adsorption domains. In both domains Cs atoms reside at stable adsorption sites, while in the region between the domains no such stable adsorption site is available. As a consequence, Cs atoms in these regions are prone to be moved by the tip leading to the observed loss of atomic resolution.

B. Intermediate coverage: $\Theta = 0.15 - 0.20$ ML

Higher Cs coverages led to an increase of the radius of the ring structure in the LEED pattern at room temperature pointing to a decrease of the average separation between Cs atoms.[52] A typical constant-current STM image of Cu(111) covered with 0.18 ML Cs is shown in Fig. 2a. We observe an almost closed Cs layer, which is disrupted by small and irregularly shaped indentations. Occasionally, these structures occur within a closed Cs layer, but most frequently they are observed at step edges. The apparent depth of the indentations depends on the applied voltage. Atomic resolution of flat areas of the Cs layer is presented in Fig. 2b. Again, we identify the bright protrusions as Cs atoms. Distances between nearest neighbors are 0.60 nm for this coverage. The corrugation of the superlattice is 0.003 nm which is considerably smaller than for $\Theta = 0.05$ ML. We attribute this observation to the Cs adatoms being more densely packed at higher coverage. Comparing with the Cu(111) substrate lattice we find a rotation angle of the adsorbate layer of 4°. We obtained the same values for the interatomic distance, the rotation angle, and the corrugation at various areas on the sample.

For Cs coverages of 0.15 ML and 0.20 ML Cs-Cs distances of 0.66 nm and 0.57 nm occur, respectively. The adsorbate layers are rotated with respect to the substrate lattice by 17° and 0°, respectively. Upon increasing the coverage the Cs adlayer becomes more and more disrupted. Instead of a closed adsorption layer numerous small Cs islands are observed (see the results for saturation coverage).

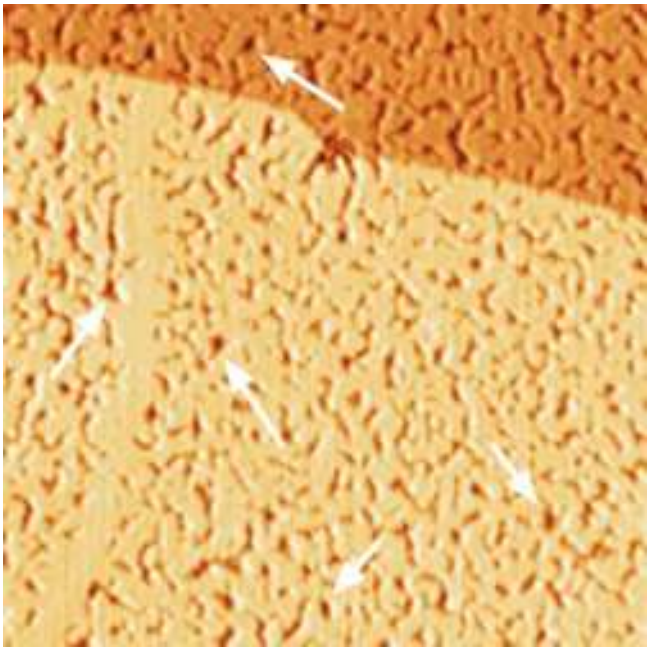

FIG. 3: (Color online) Constant-current STM image of Cu(111)-p(2 × 2)Cs at 9 K (124 nm × 124 nm, $V = 250$ mV, $I = 0.2$ nA).

C. Saturation coverage: $\Theta = 0.25$ ML

At 0.25 ML the room temperature LEED pattern reveals a clear (2 × 2) superstructure. A typical constant-current STM image of this surface at 9 K is displayed in Fig. 3. The adsorption layer is characterized by a Cs film revealing an increased number of imperfections compared to lower coverages. These imperfections, which appear as dark indentations at the given tunneling voltage exhibit a variety of sizes and shapes. We found that the dimensions of the imperfections (apparent height and lateral size) depend on the applied tunneling voltage.

IV. DISCUSSION

A. Low coverage: $\Theta = 0.05$ ML

The measured interatomic distance of 1.1 nm and the rotation angle of 23° match well a $(\sqrt{19} \times \sqrt{19})\,R\,23.4°$ commensurate phase. Stabilization of this commensurate superstructure may arise from long-range adsorbate-adsorbate interactions mediated by substrate electrons.

Lau and Kohn[58] predicted that adsorbates may interact via Friedel oscillations[59] through the fact that the binding energy of one adsorbate depends on the substrate electron density, which oscillates around the other adsorbate. Lau and Kohn later found for a two-dimensional electron gas that these interactions depend on distance, r, as $r^{-2}\cos(2\,k_{\mathrm{F}}\,r)$ where k_{F} is the Fermi vector.[60] The Cu(111) surface hosts an electronic surface state which is a model system for a two-dimensional free electron gas. The Fermi vector of this surface state is $k_{\mathrm{F}} \approx 2.2\,\mathrm{nm}^{-1}$ giving rise to Friedel oscillations with the Fermi wavelength $\lambda_{\mathrm{F}} = 2\pi k_{\mathrm{F}}^{-1} \approx 2.9\,\mathrm{nm}$.[61] Indications of such a long-range interaction between strongly bonded sulfur atoms on a Cu(111) surface have been first reported in Ref. 62. The first quantitative study of a long-range interaction mediated by a two-dimensional nearly free electron gas was reported by Repp *et al.*[63] for Cu(111)-Cu and later for Cu(111)-Cu, Cu(111)-Co, and Ag(111)-Co by Knorr *et al.*.[64] The closest separation between two Cu adatoms was 1.25 nm corresponding roughly to $\lambda_{\mathrm{F}}/2$ of the Cu(111) surface state. An atomic superlattice was also observed for adsorbed Ce atoms on a Ag(111) surface.[65] The observed 3.2 nm periodicity of the superlattice was assigned to the interaction of surface-state electrons with the Ce adatoms.

The interaction energy between adsorbates as mediated by surface state electrons was found to be[61]

$$\Delta E_{\mathrm{int}}(r) \simeq -E_{\mathrm{F}} \left(\frac{2\sin\delta_{\mathrm{F}}}{\pi}\right)^2 \frac{\sin(2k_{\mathrm{F}}r + 2\delta_{\mathrm{F}})}{(k_{\mathrm{F}}r)^2} \qquad (1)$$

where E_{F} denotes the Fermi energy measured from the bottom of the surface-state band and δ_{F} is the Fermi-level phase shift, which depends on the scatterer.[66] Inserting the experimentally observed mutual Cs distance of $(1.1 \pm 0.1)\,\mathrm{nm}$ into Eq. (1) leads to a phase shift of $\delta_{\mathrm{F}} = (0.43 \pm 0.08)\pi$. This is close to the value of $\delta_{\mathrm{F}} = (0.50 \pm 0.07)\pi$ for Cu and Co on Cu(111).[64] The similarity of these values indicates that the phase shift does not vary appreciably among these scatterers with different chemical nature. Since the value of δ_{F} in our case, *i. e.*, Cu(111)-Cs, is similar to the phase shifts obtained from the systems above, we have additional evidence that the interaction between Cs adatoms at low coverages is mediated by the Cu(111) surface state.

B. Intermediate coverage: $\Theta = 0.15 - 0.20\,\mathrm{ML}$

For the Cs superlattices observed at intermediate coverages, we do not find a coincidence of the substrate and adsorbate lattice. Consequently, on the basis of our STM investigation, we propose the adsorption layers in the intermediate coverage regime to be incommensurate. We further observed that the incommensurate adsorption phases are rotated with respect to the substrate lattice. The rotation angle of the incommensurate Cs adsorbate layers on Cu(111) as a function of the misfit $(d_{\mathrm{Cs}} - d_{2\times2})/d_{2\times2}$ is shown in Fig. 4 (circles). Here

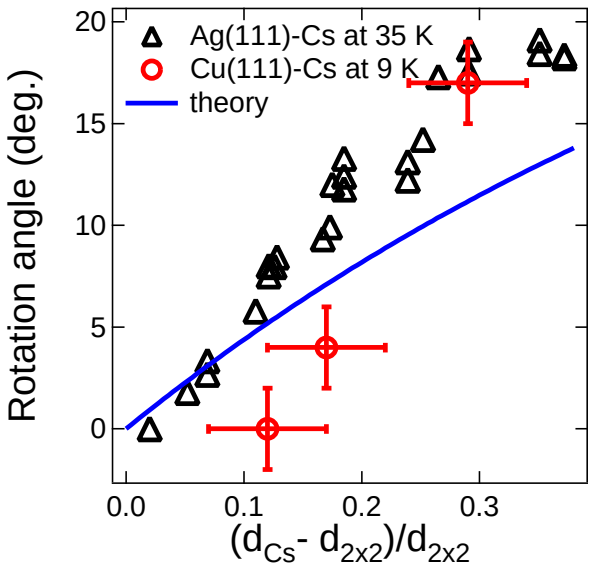

FIG. 4: (Color online) Rotation angle of a Cs adlayer on Cu(111) and Ag(111) versus misfit. Circles: Rotation angle of Cs adlayer on Cu(111), triangles: Rotation angle of Cs adlayer on Ag(111) as adapted from Ref. 20, solid line: Model calculation as described in the text.

d_{Cs} denotes the nearest-neighbor distance of the Cs adsorption layer and $d_{2\times2}$ the distance of the Cs atoms in the p(2 × 2) superstructure. The lattice constant of the Cu(111) substrate $d_{\mathrm{Cu}} \approx 0.255\,\mathrm{nm}$ leads to a nearest-neighbor distance of Cs adatoms in the p(2 × 2) superstructure of $d_{2\times2} \approx 0.511\,\mathrm{nm}$. We added data adapted from Ref. 20 displaying the rotation angles for incommensurate phases of Ag(111)-Cs at 35 K obtained by LEED (triangles). While a general trend of increasing rotation angle with increasing misfit (decreasing coverage) is observed for the two adsorbate systems, the rotation of adsorbate layers starts at larger misfits in the case of Cu(111)-Cs.

The rotation of adsorbed overlayers relative to the substrate has been observed previously for other adsorption systems.[30,67] As a consequence, several explanations of the rotational behavior of adlayers have been put forward.[20] A simple geometrical model first applied by Doering[33] proposes that the overlayer forms a higher-order commensurate phase, where the superstructure unit cell is much larger than the unit cell of the substrate surface. This leads to a large number of possible rotation angles for each misfit. It remains unclear why a specific orientation of the higher-order commensurate phase arises. Another geometrical model by Bohr and Grey[30] makes use of domain formation. The domains in question are the result of a Moiré pattern: Since the adlayer has larger interatomic spacings than the substrate there are domains where the adatoms are nearly in phase with substrate atoms; the separating areas, where the displacement is larger, are called domain walls.[67] The assumption of the model is that the layer aligns to the

substrate in such a way that the domain walls are oriented in a high-symmetry direction of the substrate or of the layer to minimize energy. Within the model by Novaco and McTague[34,35] the rotation angle of the adsorbate layer with respect to the substrate lattice is determined on the basis of a weak adsorbate-substrate interaction. Within a semiclassical approximation Novaco and McTague found the rotation angle to depend on the ratio of the longitudinal and transverse speed of sound in the adsorbate layer, c_{L} and c_{T}, respectively, and upon the ratio of the lattice constants of the substrate, $d_{2\times2}$, and the adsorbate layer, d_{Cs}:

$$\cos\theta = \frac{1+z^2(1+2\eta)}{z\,[2+\eta(1+z^2)]} \tag{2}$$

with $\eta = (c_{\mathrm{L}}/c_{\mathrm{T}})^2 - 1$ and $z = d_{2\times2}/d_{\mathrm{Cs}}$. While the lattice constants are known, little is known about the sound velocities in thin films. For alkali metals on noble metal surfaces, phonon dispersion curves were measured for Na, K and Cs on Cu(001).[68,69,70] From the phonon dispersion relations of Cs on Cu(001),[70] we know that $c_{\mathrm{L}}/c_{\mathrm{T}} = 1.2$, which leads to $\cos\theta > 1$ according to Eq. (2). We therefore calculated the ratio of sound velocities of the Cs adsorption layer by solving the two-dimensional dynamical equation

$$m\,\frac{\mathrm{d}^2 x_{n\alpha i}}{\mathrm{d}t^2} + \sum_k \Phi_{n\alpha i}^{m\beta k}\, x_{m\beta k} = 0 \quad (i = 1, 2), \tag{3}$$

where $x_{n\alpha i}$ denotes the excursion of atom α in unit cell n from equilibrium in direction i, m is the adatom mass, and

$$\Phi_{n\alpha i}^{m\beta k} = \frac{\partial^2 \Phi}{\partial x_{n\alpha i}\,\partial x_{m\beta k}} \tag{4}$$

are the coupling constants, which are calculated as the second derivative of the interaction potential. For the latter we assume a dipole potential. Numerical calculations showed that including interactions ranging further than the nearest neighbor do not change the result significantly. Since the rotation angle depends only upon the ratio of the sound velocities the actual dipole moment of Cs atoms on Cu(111) is not required for the calculation. We find $c_{\mathrm{L}}/c_{\mathrm{T}} = \sqrt{11}$ and plot θ according to Eq. (2) in Fig. 4 as a full line. The model reproduces the experimentally observed trend correctly (the larger the misfit, the larger the angle of rotation). However, the experimental result that rotation starts not until a certain misfit is exceeded is not accounted for by the model. This shortcoming of the model close to commensurate phases is known. A similar effect was reported for K and Rb adsorbed on Ag(111).[20] The authors interpreted their observation as follows: Near commensurate phases where the misfit is small the domains become larger and more adatoms are nearly in phase with substrate atoms. This leads to a stronger interaction of substrate and adlayer, locking the adlayer to the substrate orientation. A theoretical model developed by Shiba[31,32] takes this into account and predicts that for a small misfit the domain walls of the layer remain aligned to a symmetry direction of the layer up to a critical misfit. For larger misfits, the domain walls become too weak to keep the alignment, and the layer is rotated versus the substrate.

C. Saturation coverage: $\Theta = 0.25\,\mathrm{ML}$

The peculiar structure of the Cs adsorbate film as seen in constant-current STM images of Cu(111)-p(2 × 2)Cs can be explained in terms of island growth. As mentioned in the introduction alkali metal adsorption on metal surfaces goes hand in hand with the creation of dipole moments due to charge transfer processes. At low coverages the dipole-dipole interaction leads to a repulsive Cs-Cs interaction. With increasing coverage, the Cs adatoms depolarize and the repulsion decreases.[15] Reaching a sufficiently high coverage the interatomic distance is small enough to favor metallic bonds[71] and small islands are formed. With increasing size the islands eventually come close to each other and coalesce, thereby leaving behind unoccupied substrate areas.

An additional contribution to the formation of the observed Cs film structure may be due to different thermal expansion coefficients. Copper contracts by $\approx 0.3\,\%$ when cooled from room temperature to 4 K,[72] *i. e.*, the lattice constant reduces to 2.54 Å at 4 K. For (bulk) Cs published thermal expansion coefficients have not been found. Taking corresponding data for potassium[73] as an approximation for the thermal expansion coefficient of Cs we estimate that the Cs film contracts by $\approx 2\,\%$ upon cooling from room temperature to 4 K. Consequently, the Cs lattice constant reduces to ≈ 5 Å. Supposing that at room temperature the Cs layer covers the complete surface, which is corroborated by our room temperature STM and LEED studies, the different contraction of the Cs adsorption layer and the Cu surface leads to a coverage of 96 % of the surface at 4 K, leaving 4 % of the surface uncovered. Analysing a variety of constant-current STM images of the p(2×2)Cs superstructure we find that $\approx 82\,\%$ of the surface was covered. As a consequence, the different thermal contraction of the Cs adsorption layer and the Cu surface may contribute to the observed layer structure although cannot explain the entire effect.

V. SUMMARY

We used low-temperature STM to investigate Cu(111)-Cs at various Cs coverages. For very low coverages the Cs adsorption layer reveals hexagonal order with a nearest-neighbor distance of 1.1 nm. We interpret this adsorption phase as a commensurate superstructure stabilized by long-range interactions mediated by surface state electrons. For higher coverages we find incommensurate Cs superlattices, which are rotated with respect

to the Cu(111) substrate lattice. In contrast to the high degree of order at low and intermediate coverages, the p(2 × 2)Cs superstructure at saturation coverage exhibits a fairly large defect density.

Financial support by the Deutsche Forschungsgemeinschaft via the Schwerpunktprogramm 1093 is gratefully acknowledged.

* Electronic address: kroeger@physik.uni-kiel.de

[1] J. E. Ortega, E. M. Oellig, J. Ferron, and R. Miranda, Phys. Rev. B **36**, 6213 (1987).
[2] M. Tikhov, G. Rangelov, and L. Surnev, Surf. Sci. **231**, 280 (1990).
[3] G. Faraci and A. R. Pennisi, Surf. Sci. **409**, 46 (1998).
[4] S. Y. Davydov, Appl. Surf. Sci. **140**, 58 (1999).
[5] J. B. Taylor and I. Langmuir, Phys. Rev. **44**, 423 (1933).
[6] A. H. Somer, *Photoemissive Materials* (Wiley, New York, 1968).
[7] J. P. Muscat and D. M. Newns, Prog. Surf. Sci. **9**, 1 (1978).
[8] N. D. Lang, in *Physics and Chemistry of Alkali Metal Adsorption*, edited by H. P. Bonzel, A. M. Bradshaw, and G. Ertl (Elsevier, Amsterdam, 1989).
[9] M. Bauer, S. Pawlik, and M. Aeschlimann, Phys. Rev. B **55**, 10040 (1997).
[10] S. Ogawa, H. Nagano, and H. Petek, Phys. Rev. Lett. **82**, 1931 (1999).
[11] A. G. Borisov, J. P. Gauyacq, A. K. Kazansky, E. V. Chulkov, V. M. Silkin, and P. M. Echenique, Phys. Rev. Lett. **86**, 488 (2001).
[12] J. P. Gauyacq, A. G. Borisov, and A. K. Kazansky, Appl. Phys. A **78**, 141 (2004).
[13] C. Corriol, V. M. Silkin, D. Sanchez-Portal, A. Arnau, E. V. Chulkov, P. M. Echenique, T. von Hofe, J. Kliewer, J. Kröger, and R. Berndt, Phys. Rev. Lett. **95**, 176802 (2005).
[14] R. D. Diehl and R. McGrath, Surf. Sci. Rep. **23**, 43 (1996).
[15] K. Wandelt, in *Physics and Chemistry of Alkali Metal Adsorption*, edited by H. P. Bonzel, A. M. Bradshaw, and G. Ertl (Elsevier, Amsterdam, 1989).
[16] W. C. Fan and A. Ignatiev, Phys. Rev. B **37**, 5274 (1988).
[17] J. Cousty and R. Riwan, Surf. Sci. **204**, 45 (1988).
[18] D. Tang, D. McIlroy, X. Shi, C. Su, and D. Heskett, Surf. Sci. **255**, L497 (1991).
[19] Z. Y. Li, K. M. Hock, and R. E. Palmer, Phys. Rev. Lett. **67**, 1562 (1991).
[20] G. S. Leatherman and R. D. Diehl, Phys. Rev. B **53**, 4939 (1996).
[21] T. Masuda, C. J. Barnes, P. Hu, and D. A. King, Surf. Sci. **276**, 122 (1992).
[22] D. K. Flynn-Sanders, K. D. Jamison, J. V. Barth, J. Wintterlin, P. A. Thiel, G. Ertl, and B. J. Behm, Surf. Sci. **253**, 270 (1991).
[23] P. Kaukasoina, M. Lindroos, R. D. Diehl, D. Fisher, S. Chandavarkar, and I. R. Collins, J. Phys.: Condens. Matter **5**, 2875 (1993).
[24] D. Fisher and R. D. Diehl, Phys. Rev. B **46**, 2512 (1992).
[25] N. J. Wu, Z. P. Hu, and A. Ignatiev, Phys. Rev. B **43**, 3805 (1991).
[26] G. Pirug and H. P. Bonzel, Surf. Sci. **194**, 159 (1988).
[27] D. L. Doering and S. Semancik, Surf. Sci. **175**, L730 (1986).
[28] D. L. Doering and S. Semancik, Phys. Rev. Lett. **53**, 66 (1984).
[29] G. Besold, T. Schaffroth, K. Heinz, G Schmidt, L. Hammer, K. Heinz, and K. Müller, Surf. Sci. **189/190**, 252 (1987).
[30] F. Grey and J. Bohr, in *Phase Transitions in Surface Films 2*, edited by H. Taub, G. Torzo, H. J. Lauter, and S. C. Fain, Jr. (Plenum Press, New York, 1991), p. 83.
[31] H. Shiba, J. Phys. Soc. Jpn. **46**, 1852 (1979).
[32] H. Shiba, J. Phys. Soc. Jpn. **48**, 211 (1980).
[33] D. L. Doering, J. Vac. Sci. Technol. A **3**, 809 (1985).
[34] A. D. Novaco and J. P. McTague, Phys. Rev. Lett. **38**, 1286 (1977).
[35] J. P. McTague and A. D. Novaco, Phys. Rev. B **19**, 5299 (1979).
[36] J. N. Andersen, E. Lundgren, R. Nyholm, and M. Qvarford, Surf. Sci. **289**, 307 (1993).
[37] H. Brune, J. Wintterlin, R. J. Behm, and G. Ertl, Phys. Rev. B **51**, 13592 (1995).
[38] W. Berndt, D. Weick, C. Stampfl, A. M. Bradshaw, and M. Scheffler, Surf. Sci. **330**, 182 (1995).
[39] R. Nyholm, E. Lundgren, A. Beutler, J. N. Andersen, and D. Heskett, Surf. Sci. **370**, 311 (1997).
[40] N. Fischer, S. Schuppler, T. Fauster, and W. Steinmann, Surf. Sci. **314**, 89 (1994).
[41] H. Tochihara and S. Mizuno, Surf. Sci. **279**, 89 (1992).
[42] T. Aruga, H. Tochihara, and Y. Murata, Surf. Sci. **175**, L725 (1986).
[43] S. Modesti, C. T. Chen, Y. Ma, G. Meigs, P. Rudolf, and F. Sette, Phys. Rev. B **42**, 538 (1990).
[44] J. Neugebauer and M. Scheffler, Phys. Rev. Lett. **71**, 577 (1993).
[45] C. Stampfl, J. Neugebauer, and M. Scheffler, Surf. Sci. **307-309**, 8 (1994).
[46] S. Andersson and J. B. Pendry, Solid States Commun. **16**, 563 (1975).
[47] J. E. Demuth, D. W. Jepsen, and P. M. Marcus, J. Phys. C (Solid States Phys.) **8**, L25 (1975).
[48] C. von Eggeling, G. Schmidt, G. Besold, L. Hammer, K. Heinz, and K. Müller, Surf. Sci. **221**, 11 (1989).
[49] S. Aminpirooz, A. Schmalz, L. Becker, N. Pangher, J. Haase, M. M. Nielsen, D. R. Batchelor, E. Bøgh, and D. L. Adams, Phys. Rev. B **46**, 15594 (1992).
[50] U. Muschiol, P. Bayer, K. Heinz, W. Oed, and J. B. Pendry, Surf. Sci. **275**, 185 (1992).
[51] S. Mizuno, H. Tochihara, and T. Kawamura, Surf. Sci. **293**, 239 (1993).
[52] S. Å. Lindgren, L. Walldén, J. Rundgren, P. Westrin, and J. Neve, Phys. Rev. B **28**, 6707 (1983).
[53] M. Kerkar, D. Fisher, D. P. Woodruff, R. G. Jones, R. D. Diehl, and B. Cowie, Phys. Rev. Lett. **68**, 3204 (1992).
[54] D. Fisher, S. Chandavarkar, I. R. Collins, R. D. Diehl, P. Kaukasoina, and M. Lindroos, Phys. Rev. Lett. **68**, 2786 (1992).
[55] S. Schwegmann and H. Over, Surf. Sci. **360**, 271 (1996).
[56] W. C. Fan and A. Ignatiev, J. Vac. Sci. Technol. A **6** 735 (1988).

[57] SAES Getters, Cologne, Germany.
[58] K. H. Lau and W. Kohn, Surf. Sci. **65**, 607 (1977).
[59] J. Friedel, Nuovo Cimento, Suppl. **7**, 287 (1958).
[60] K. H. Lau and W. Kohn, Surf. Sci. **75**, 69 (1978).
[61] P. Hyldgaard and M. Persson, J. Phys.: Condens. Matter **12**, L13 (2000).
[62] E. Wahlström, I. Ekvall, H. Olin, and L. Walldén, Appl. Phys. A **66**, S1107 (1998).
[63] J. Repp, F. Moresco, G. Meyer, and K.-H. Rieder, Phys. Rev. Lett. **85**, 2981 (2000).
[64] N. Knorr, H. Brune, M. Epple, A. Hirstein, M. A. Schneider, and K. Kern, Phys. Rev. B **65**, 115420 (2002).
[65] F. Silly, M. Pivetta, M. Ternes, F. Patthey, J. P. Pelz, and W.-D. Schneider, Phys. Rev. Lett. **92**, 016101 (2004).
[66] G. Hörmandinger and J. B. Pendry, Phys. Rev. B **50**, 18607 (1994).
[67] F. Grey and J. Bohr, Europhys. Lett. **18**, 717 (1992).
[68] G. Benedek, J. Ellis, A. Reichmuth, P. Ruggerone, H. Schief and J. P. Toennies, Phys. Rev. Lett. **69**, 2951 (1992).
[69] E. Hulpke, J. Lower, and A. Reichmuth, Phys. Rev. B **53**, 13901 (1996).
[70] G. Witte and J. P. Toennies, Phys. Rev. B **62**, R7771 (2000).
[71] S. Å. Lindgren and L. Walldén, Phys. Rev. B **22**, 5967 (1980).
[72] G. K. White, *Experimental Techniques in Low-Temperature Physics* (Oxford University Press, 1968).
[73] D. R. Schouten and C. A. Swenson, Phys. Rev. B **10**, 2175 (1974).